BULLETIN OF THE POLISH ACADEMY OF SCIENCES
TECHNICAL SCIENCES
Vol. 57, No. 4, 2009

High efficiency contactless energy transfer system with power electronic resonant converter

A.J. MORADEWICZ[1] and M.P. KAZMIERKOWSKI[2*]

[1] Electrotechnical Institute IEl, 28 M. Pożaryskiego St., 04-703 Warsaw, Poland
[2] Institute of Control and Industrial Electronics, Warsaw University of Technology, 75 Koszykowa St., 00-662 Warsaw, Poland

Abstract. A novel Inductive Contactless Energy Transfer (ICET) system is presented in this paper. The energy is transferred using a rotatable air gap transformer and a power electronic converter. To minimize total losses of the system a series resonant circuit is applied, assuring zero current switching condition for IGBT power transistors. The analytical expression of the transfer dc voltage gain is given and discussed. The developed ICET system is characterized by high efficiency and fast FPGA based controller and protection system. The resonant frequency is adjusted by extreme regulator which follows instantaneous value of primary peak current. Simulated and experimental results which verify and illustrate operation of developed 3 kW laboratory model are presented.

Key words: inductive contactless energy transfer, series resonant converter, FPGA control.

1. Introduction

The contactless energy transfer systems have been recently gaining popularity and investigated widely [1–16]. This innovative technology creates new possibilities to supply mobile devices with electrical energy because elimination of cables, and/or slip-rings as well as plugs and sockets increases reliability and maintenance-free operation of such critical systems as in aerospace, biomedical, electric vehicles and robotics applications. The core of contactless energy transfer system is inductive or capacitive coupling and high switching frequency power electronic converter. The capacitive coupling is used in low power range (sensor supply systems) whereas inductive coupling allows transferring power from a few mW up to hundred kW [1, 4].

This paper reports on a new developed Inductive Contactless Energy Transfer (ICET) system with a rotatable air gap transformer and IGBT transistors based resonant power electronic converter. Thanks to the careful design of all system-components, the high total efficiency (93%) is achieved. Other important features of the presented ICET system are: operation of high-switching frequency IGBT transistor based resonant converter at zero current switching (ZCS) conditions, low cost single board FPGA based controller, reliable and fast operation, robustness to magnetic coupling factor changes of the main circuit. Simulation and experimental results of 3kW prototype system operated with 60 kHz switching frequency are presented.

2. Topology of Inductive contactless energy transfer (ICET) system

The topology of the investigated experimental ICET system is shown in Fig. 1(a). The core of the system is a rotatable transformer with adjustable air gap. This air gap can be enlarged, for testing purposes, up to 30 mm. At the energy feeding input there are: a three-phase diode rectifier and a full bridge IGBT converter. At the secondary side a load module R_o with diode bridge rectifier is connected. This solution has the following advantages: secondary circuits can be movable relatively to primary, control and power supply system is located on the primary side and is electrically separated from the secondary circuit. The system can also be easily expanded by connecting on secondary DC output DC/AC inverters for variable frequency three-phase loads [10, 16, 17]. For high power applications the supply diode rectifier can be replaced by high switching frequency boost rectifier operating with unity power factor [18].

In conventional applications a transformer is used for galvanic insulation between source and load, and its operation is based on high magnetic coupling factor between primary and secondary windings. Due to the air gap between two half-cores, the ICET transformers operate under much lower magnetic coupling factor. As a result the main inductance L_{12} is very small whereas leakage inductances L_{11} and L_{22} are large in comparison with conventional transformers. Consequently, the increase of magnetizing current causes higher conducting losses and also, winding losses increase because of large leakage inductances. To minimize the above disadvantages of ICET transformers several power conversion topologies have been proposed which can be classified in the following categories: the flyback, resonant, quasi-resonant and self-resonant [16]. The common for all these topologies is that they utilize the energy stored in the transformer. In this work resonant soft switching technique in full bridge topology has been used. To build up resonant circuits two methods of transformer leakage inductances compensation can be applied: S-series or P-parallel giving four basic circuits: SS, SP, PS, and PP (first letter denotes primary and second a secondary

*e-mail: mpk@isep.pw.edu.pl

a)

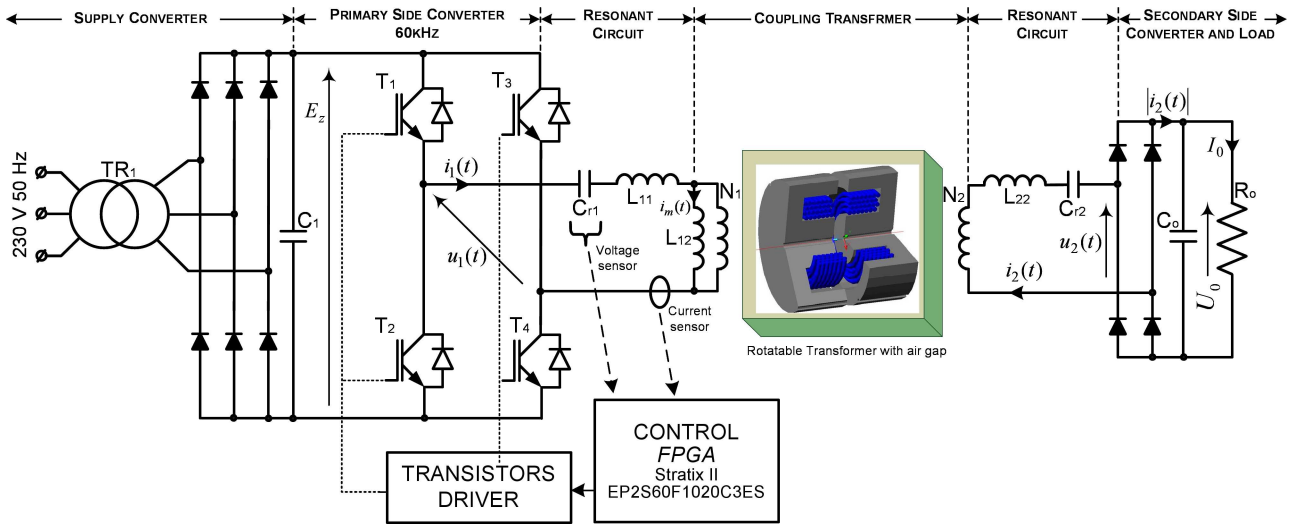

b)

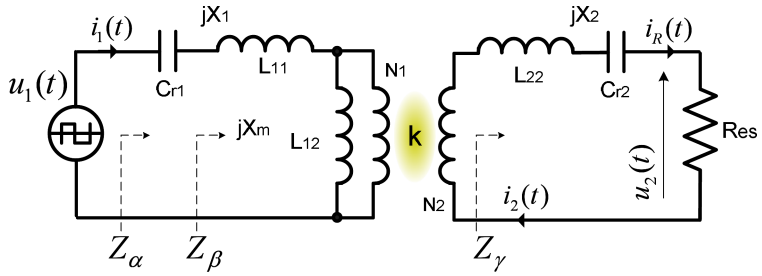

Fig. 1. (a) Circuit topology of developed Inductive Contactless Energy Transfer (ICET) system, (b) Equivalent circuit for fundamental harmonic

compensation). PS and PP require an additional series inductor to regulate the inverter current flowing into the parallel resonant circuit. This additional inductor increases Electro-Magnetic Compatibility (EMC) problems and total cost of ICET system. Therefore, only SS and SP circuits have been considered.

3. Analysis of compensation circuits

Assuming the same numbers of primary and secondary winding $N_1 = N_2$, the inductances of presented transformer can be described as follows:

$$\begin{array}{ccc} L_1 = L_{11} + L_{12} & & L_1 = L_{11} + L_{12} \\ L_2 = L_{22} + n^2 L_{12} & \Rightarrow & L_2 = L_{22} + L_{12} \\ M = nL_{12} & & M = L_{12} \end{array} \tag{1}$$

where

$$L_1 = L_2 = L,$$

$$L_{11} = L_{22} = L - M = \frac{1-k}{k} M, \tag{2}$$

$$k = M/L, \qquad n = \frac{N_2}{N_1}.$$

If the fundamental component of $u_2\ (t)$ is in phase with $i_2\ (t)$, the output rectifier with capacitive filter behaves as load resistance transformer. The value of this resistance is equal to [1]:

$$R_{es} = \frac{8U_0}{\pi^2 I_0} = 0.8106 \cdot R_o. \tag{3}$$

Impedance of secondary side in case of chosen compensation circuits is:

– for series compensation:

$$Z_\gamma = R_{es} + jX_2, \tag{4}$$

– for parallel compensation:

$$Z_\gamma = \left\{ j\omega L_{11} + 1/\left(j\omega \cdot C_{r2} + \frac{1}{R_{ep}} \right) \right. . \tag{5}$$

The equations for component impedance and reactance, shown at various points in Fig. 1(b) can be written as:

$$Z_\beta = \frac{jX_m \cdot Z_\gamma}{jX_m + Z_\gamma} \tag{6}$$

$$Z_\alpha = jX_1 + Z_\beta, \tag{7}$$

$$X_1 = \omega_s L_{11} - \frac{1}{\omega_s C_{r1}}, \tag{8}$$

$$X_2 = \omega_s L_{22} - \frac{1}{\omega_s C_{r2}}, \tag{9}$$

$$X_m = \omega_s M, \tag{10}$$

where $\omega_s = 2\pi f_s$ – operation inverter frequency.

The voltage transfer function of ICET system for SS compensation circuits in Fig. 1(b) is:

$$G_V = \left| \frac{Z_\beta}{Z_\alpha} \frac{R_{es}}{Z_\gamma} \right|. \tag{11}$$

From Eqs. (3) to (11), the resulting equation of the transfer gain G_V express as:

$$G_V = \left[\left(1 + \frac{X_1}{X_m} \right)^2 + \left(\frac{X_1 + X_2 + \dfrac{X_1 \cdot X_2}{X_m}}{R_{es}} \right)^2 \right]^{-\frac{1}{2}}. \tag{12}$$

From Eq. (12) follows that G_V is unity at compensated frequency, even though the leakage inductances of the rotating transformer in ICET system are very large. Where $\omega_0 = 2\pi f_0$ – resonant frequency – (compensated frequency), is derived for condition $X1 = X_2 = 0$

$$\omega_o = 1/\sqrt{L_r C_r} = 1/\sqrt{L_{11} C_{R1}} = 1/\sqrt{L_{22} C_{R2}}. \tag{13}$$

Based on Eqs. (7, 8 and 13) the expression for X_1 and X_2 can be rewritten by:

$$X_1 = \omega_s L_{11} \left(1 - \frac{1}{\omega^2} \right), \tag{14}$$

$$X_2 = \omega_s L_{22} \left(1 - \frac{1}{\omega^2} \right), \tag{15}$$

where

$$\omega = \omega_s / \omega_o. \tag{16}$$

Because of used two half-cores and large air gap, the ICET transformer operates under low and variable magnetic coupling factor k. Therefore, the voltage gain G_V can be expressed in terms of coupling factor k. For simplification we assume that the configurations of primary and secondary transformer windings are identical. From Eqs. (12) to (16) the voltage gain function can be rewritten as:

$$G_V = \sqrt{\left(1 + \frac{1-k}{k} \left(1 - \frac{1}{\omega^2} \right) \right)^2 + \left(Q_{ac} \left(\omega - \frac{1}{\omega} \right) \left(1 + \frac{1-k}{2k} \left(1 - \frac{1}{\omega^2} \right) \right) \right)^2}, \tag{17}$$

where circuit quality factor for SS compensation topology is:

$$Q_{ac} = \frac{\omega \left(L_{11} + L_{22} \right)}{R_{es}} = \frac{\omega L_r}{R_{es}}. \tag{18}$$

The analytical results of the voltage gain function based on Eq. (17) are illustrated in Fig. 2. The calculations were performed versus the normalized angular frequency ω, for two values of coupling factor k and various Q_{ac} as parameter. It can be seen that the curves of voltage transfer function G_V for $k = 0.2$ and 0.8 are similar except for a small deviation in low circuit quality factor Q_{ac}. For the output-voltage regulation, the feedback control should be applied selecting the desirable operation range from three different regions A, B and C of the voltage transfer function G_V presented in Fig. 2. Regions A or C are able to unambiguous control the output voltage since the G_V is a monotonic function of switching frequency. The range C is favorable because the voltage transfer function for each load conditions is much less sensitive than in the Range A. Moreover, when increasing switching frequency, the changes in output voltage are very fast. This fact is important in control system, for example when dangerous state is detecting ($\omega_s < \omega_o$).

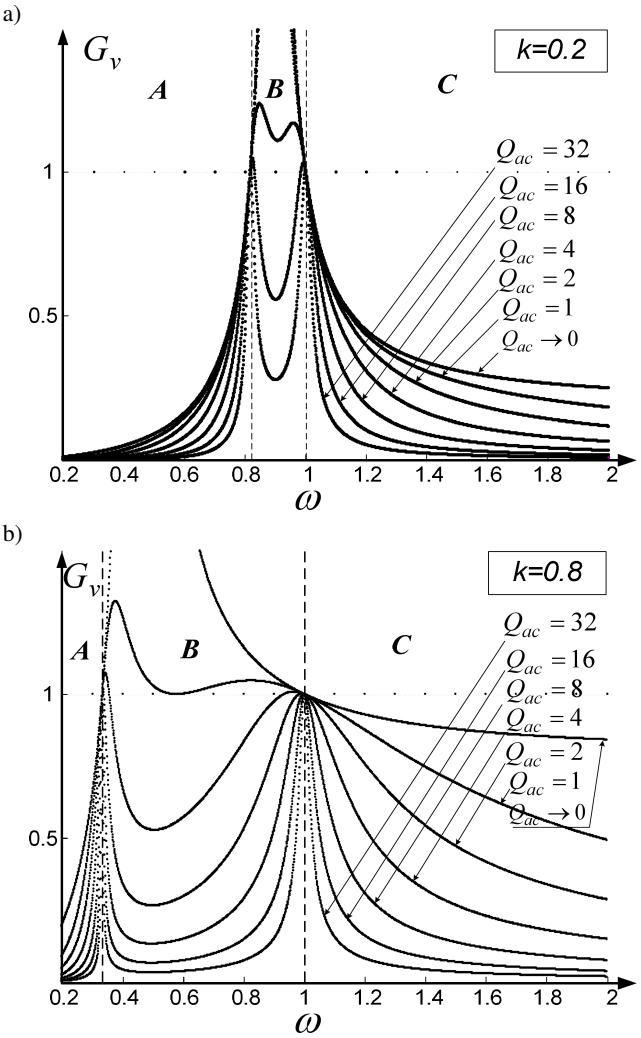

Fig. 2. Illustration of transfer dc voltage gain G_v versus normalized frequency in ICET system for SS compensation circuit. a) $k = 0.2$, b) $k = 0.8$

The required resonant capacitors values for desired resonant frequency can be expressed as follows:
– for series secondary compensation

$$C_{r1} = \frac{L_{22}}{L_{11}} C_{r2} = C_{r2|L_{11}=L_{22}}, \tag{19}$$

– for parallel secondary compensation

$$C_{r1} = \frac{L_{22}^2 \cdot C_{r2}}{L_{11} \cdot L_{22} - \left(k \cdot L_{11} \cdot L_{22} \right)^2} = {}_{|L_{11}=L_{22}|} = \frac{1}{1-k^2} C_{r2}. \tag{20}$$

An important advantage of SS compensation circuit is that primary capacitance is independent of either magnetic coupling factor or the load. In contrast the SP circuit depends on coupling factor and requires higher value of capacitance for stronger magnetic coupling.

4. Control and protection scheme

The block scheme of the ICET control and protection system implemented in FPGA Stratix II is shown in Fig. 3. The clock frequency of the FPGA is 100 MHz and the resonant switching frequency is 60 kHz. The inverter output current i_1 is measured and sent to A/D converters via operation amplifiers. A 12-b A/D converter, AD9433 is used in the designed system. The analog input signal is 5 V (V_{DD}), hence maximum amplitude corresponds to 2.5 V. The FPGA device is Stratix II EP2S60F1020C3ES.

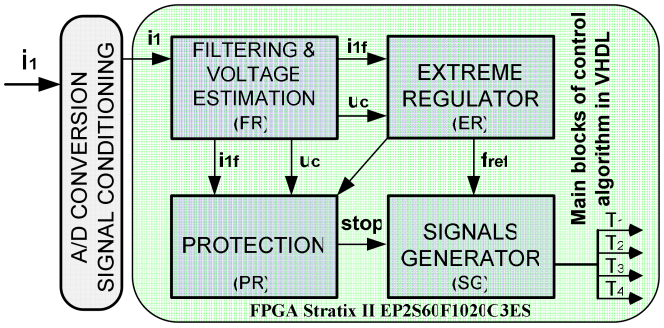

Fig. 3. Block scheme of the ICET control and protection system

The inverter output current i_1 is measured and sent to A/D converters via a conditioning circuit. A 12-b A/D converter, AD9433 is used in the designed system. The typical analogy input signal is 5 V (V_{DD}), hence maximum of amplitude correspond to 2.5 V. The FPGA device is Stratix II EP2S60F1020C3ES.

To attenuate noise in current input signal (i_1') from measurements block (Fig. 3) a digital recursive filtering algorithm has been applied. Additionally, for limitation and protection purposes the primary capacitor voltage u_{cr1} is estimated from the converter output current according to following equation:

$$u_{Cr1}(t) = \frac{i_1(t)}{\omega C_{r1}}. \tag{21}$$

The filtered signal i_{1f} is used in extreme regulator (ER). Also, the sign of the primary current i_{1s} is calculated based on filtered value i_1'. The ER includes reversible counter which determinates converter switching frequency f_{ref}. The signal f_{ref} is delivered to the signal generator (SG) which generates gate pulses for IGBT power transistors $T_1 \ldots T_4$. Also, dead time compensation is implemented in this block (SG).

To guarantee stable operations, the regulator ER in every N-period sequence searches the highest current amplitude i_{1fm} and, after comparison with previous data, adjusts reference value of switching frequency f_{ref}. Additionally, the input signals i_{1f} and u_c are delivered to protection block (PR). The PR block continuously watch up these signals and blocks IGBT gate pulses $T_1 \ldots T_4$ in case when limit values $i_{1f(lim)}$ and $u_{c(lim)}$ are achieved. Current limit during the converter start-up, is implemented by regulator (ER) which sets the switching frequency higher then resonant frequency $f_{ref} > f_o$ and then in every N-period sequence reduces f_{ref} in such a way that the current amplitude is kept below the limit. If the voltage and/or current amplitude reaches the limit value:

$$i_{1f(N)} = i_{1f(lim)},$$

$$u_{c(N)} = u_{c(lim)},$$

the regulator (ER) increases converter switching frequency. This effect produces an increment of the circuit impedance and as consequence the current and capacitor voltage will be reduced. The period N of regulator operation has been selected experimentally $N = 7$.

The control and protection algorithm is implemented in the VHDL software. The flow diagram of the extreme regulator (ER) is shown in Fig. 4.

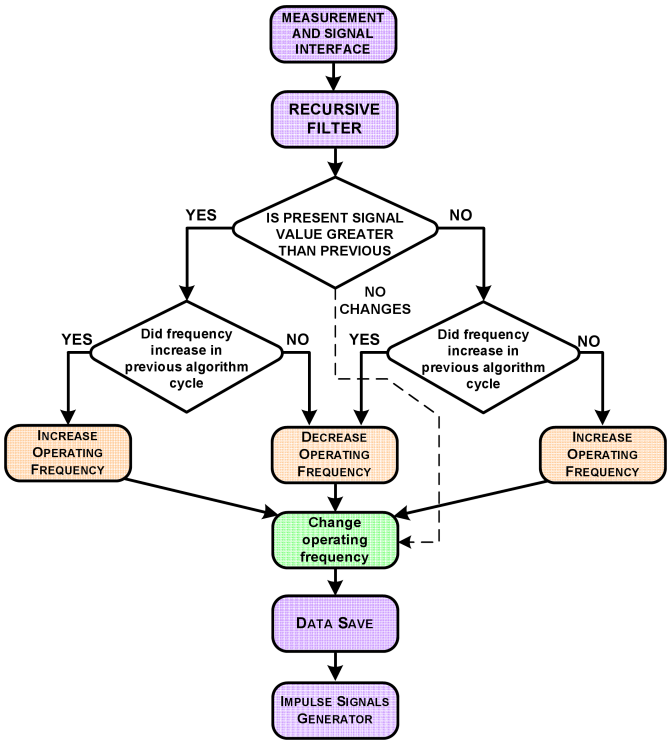

Fig. 4. Extreme regulator algorithm for primary peak current mode

5. Simulated and experimental verification

The performance of developed ICET system has been verified by PSPICE simulation and measurements on 3 kW experimental laboratory set-up (Fig. 5). The basic parameters of rotatable transformer and resonant converter are given in Table 1 and Table 2, whereas measured self inductances of transformers windings versus air gap width are shown in Fig. 6.

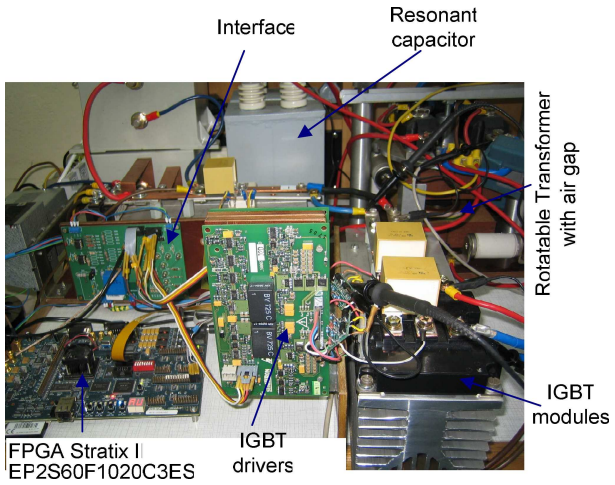

Fig. 5. View of laboratory setup of 3kW contactless power supply system with rotatable transformer and series resonant IGBT inverter

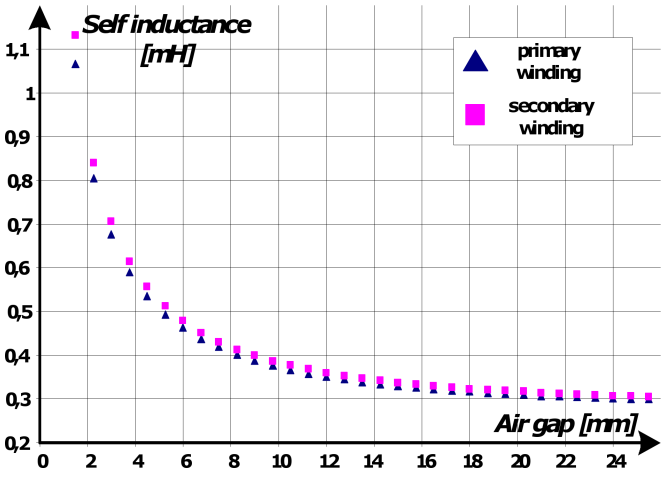

Fig. 6. Measured self inductance primary and secondary winding of rotating transformer in laboratory model

Table 1
Parameters of rotatable transformer and resonant circuit

Parameter	Value	Unit
N_1 and N_2	32	coils
L_{11}	166.5	μH
L_{12}	203.5	μH
L_{22}	166.5	μH
M	203.5	μH
k	0.55	–
C_{R1} and C_{R2}	63	nF
Air gap	10.5	mm

Table 2
Parameters of resonant converter

Parameter	Value	Unit
Power Module	SKM100GB124D	
Voltage	1200	V
Current	150	A
Dead Time	1	μs
C_1	1000	μF
C_{R1}	63	nF
C_{R2}	63	nF
C_O	100	μF

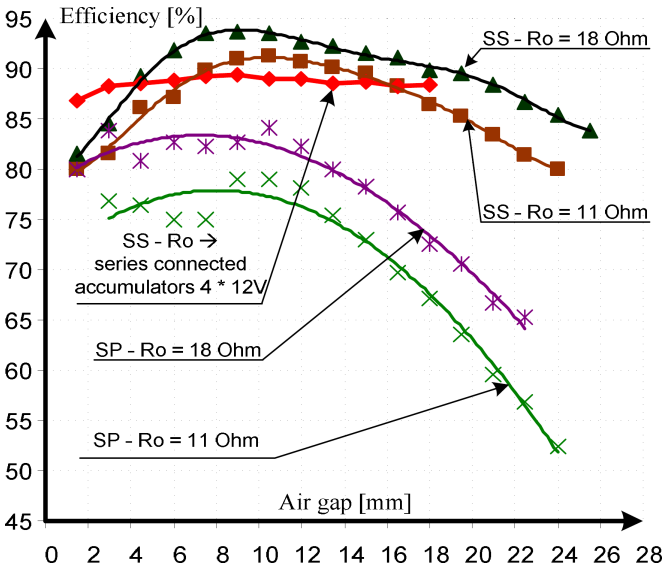

Fig. 7. Efficiency versus air gap width of the experimental ICET system

Figure 7 shows total dc-dc measured input-output efficiency of the ICET laboratory model system versus transformer air gap width and the load resistance. Note, that for higher load resistances, in both compensation circuits, higher efficiency is achieved. However, the efficiency of ICET system with *SP* compensation is about 10% lower then with SS circuit, for the same circuit parameters.

Figures 8 and 9 show PSPICE simulated and experimental measured oscillograms of basic waveforms in the steady-state operation of resonant converter. The load resistance was 10 Ω and transformer air gap width 3 and 25.5 mm in Fig. 8a and Fig. 9, respectively. Operation mode above resonant frequency for 3 mm transformer air gap width is shown in Fig. 8b. Note that at resonant frequency power IGBT transistors operate at Zero Current Switching (ZCS) conditions and power factor achieves a value of 0.912 for power level 2.52 kW (Fig. 9). Above resonant frequency (Fig. 8b) power transistor operate at non ZCS conditions, with low power factor value of 0.279 and power level 137 W. The power flow is controlled by detuned operation.

Investigation of operation at resonant frequency with different transformer air gap width has shown that system is well synchronized by extreme regulator and operates properly for magnetic coupling factor changes from 0.2 till 0.8.

Note that for higher load resistances higher efficiency can be achieved, but the circuit becomes more sensitive to magnetic coupling factor changes.

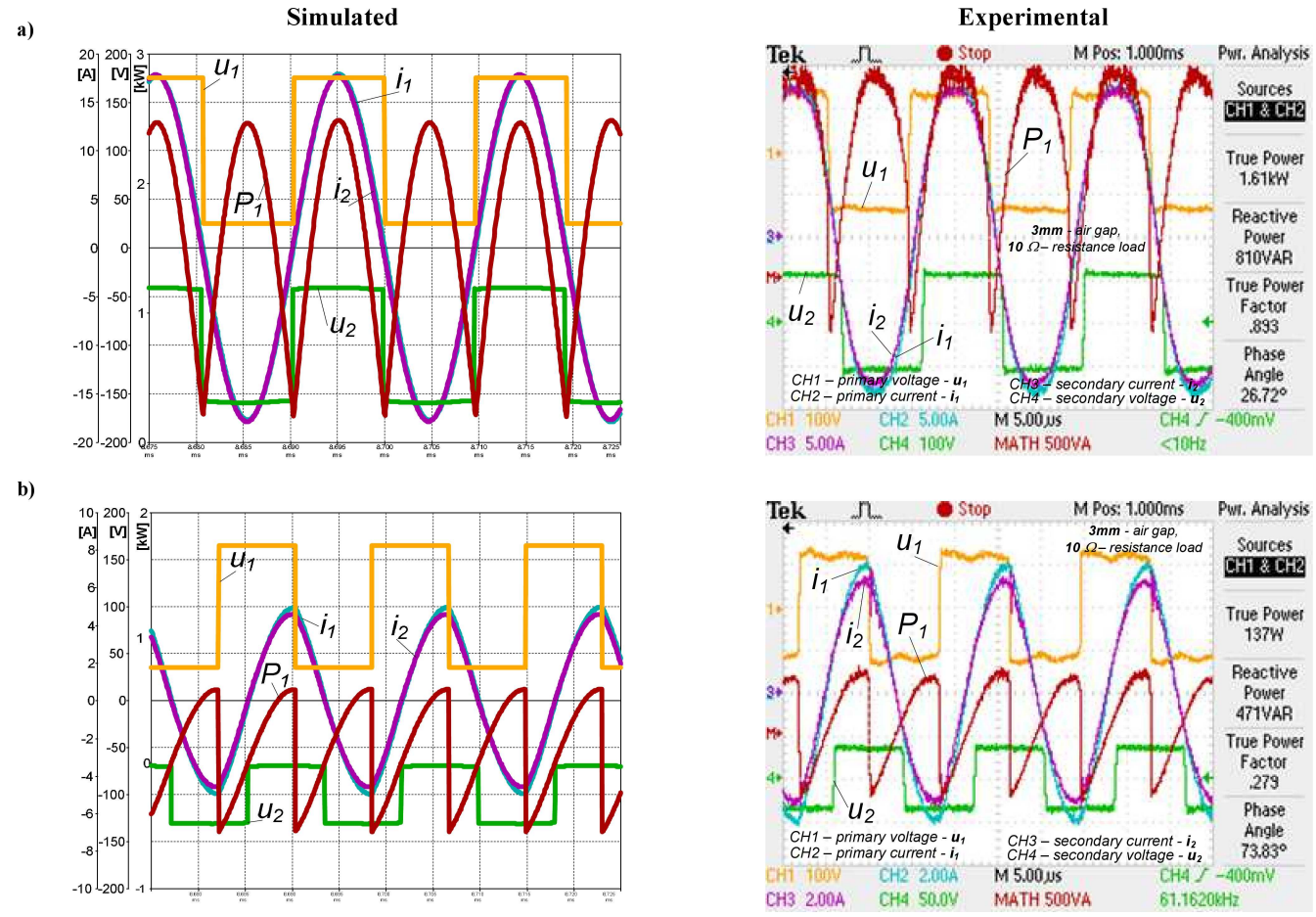

Fig. 8. Converter operation at steady-state: a) at resonant frequency, b) above resonant frequency. From the top: voltages u_1, u_2, currents i_1, i_2 and primary side power P_1. Air gap length 3 mm, load resistance 10 Ω

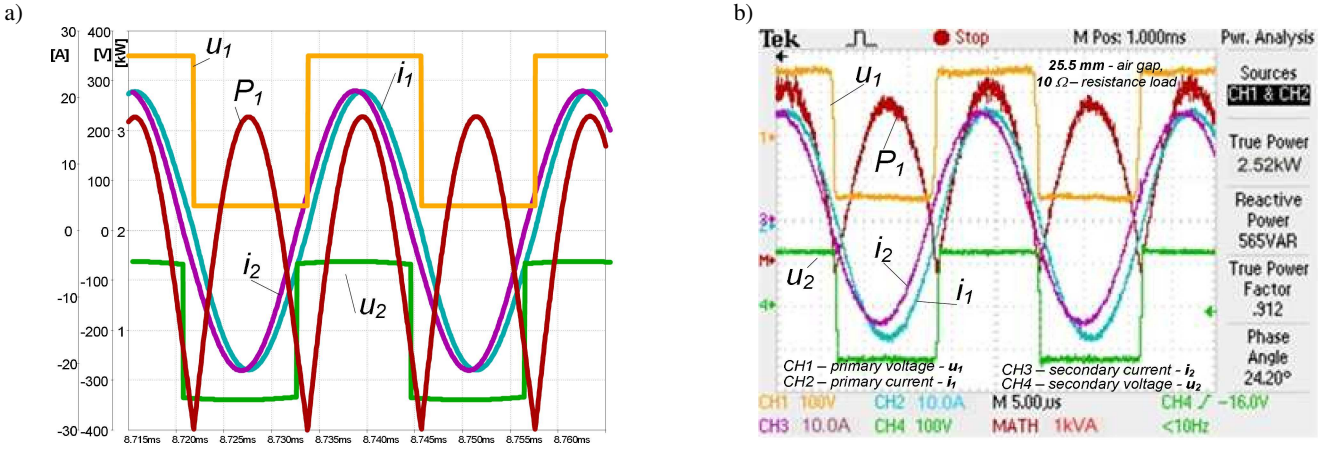

Fig. 9. Converter operation at steady-state: a) at resonant frequency, b) above resonant frequency. From the top: voltages u_1, u_2, currents i_1, i_2 and primary side power P_1. Air gap length 25.5 mm, load resistance 10 Ω

6. Conclusions

This paper presents an Inductive Contactless Energy Transfer (ICET) system with rotatable air gap transformer and series resonant power electronic converter operating at 60 kHz switching frequency.

The control and the protection system have been implemented in FPGA Stratix II EP2S60F family. To compensate for high leakage inductance of the rotatable transformer when a large air gap is used and to minimize converter switching losses, the series resonant capacitive circuit has been used in primary and secondary side. The resonant frequency is adjusted by extreme regulator which follows the instantaneous value of primary peak current and guaranties zero current switching (ZCS) conditions for power IGBT transistors of the inverter. This reduces switching losses consid-

erably and increase overall system efficiency. Theoretically, there is no power transfer limit, even with low magnetic coupling factor, if the system operates at the resonant frequency of secondary current, with compensated primary winding conditions. Additionally, resonant frequency of primary current should by equal to secondary. From (19) it can be concluded that in *SS* compensation topology both resonant capacitances are equal, if $L_{11} = L_{22}$. The design procedure has been verified by simulation and experimental results measured on the 3 kW laboratory set-up. The total efficiency achieves 93% for transformer with *10 mm* air gap width.

The developed ICET with a rotatable transformer is constructed mainly for robotics and manipulators, however, the described design and control methodology has a general validity and can be applied for a wide class of contactless power supply with core or core-less transformers.

REFERENCES

[1] Ch. Apneseth, D. Dzung, S. Kjesbu, G. Scheible, and W. Zimmermann, "Introduction wireless proximity switches", *ABB Review* 4, 42–49 (2002).

[2] A. Esser and H.Ch. Skudelny, "A new approach to power supply for robots", *IEEE Trans. on Ind. Applications* 27 (5), 872–875 (1991).

[3] J. Hirai, T.W. Kim, and A. Kawamura, "Study on intelligent battery charging using inductive transmission of power and information", *IEEE Trans. on Power Electronics* 15, 2, 335–344 (2000).

[4] M. Jufer, "Electric drive system for automatic guided vehicles using contact-free energy transmission", *Electrotechnical Review* 84 (9), 35–39 (2008), (in Polish).

[5] J. Lastowiecki and P. Staszewski, "Sliding transformer with long magnetic circuit for contactless electrical energy delivery to mobile receivers, *IEEE Trans. on Industrial Electronics* 53, 6, 1943–1948 (2006).

[6] J.T. Matysik, "A new method of integration control with instantaneous current monitoring for class D", *IEEE Trans. on Industrial Electronics* 53, 5, 1561–1576 (2006).

[7] R. Mecke and C. Rathage, "High frequency resonant converter for contactless energy transmission over large air gap", *Proc. IEEE-PESC* 1, 1737–1743 (2004).

[8] R. Miśkiewicz and A. Moradewicz, "Contactless power supply for notebooks", *Electrotechnical Review* 85 (3), 8–14 (2009), (in Polish).

[9] A. Moradewicz, "Contactless energy transmission system with rotatable transformer – modeling, analyze and design", *PhD-Thesis*, Electrotechnical Institute (IEl), Warsaw, Poland, 2008.

[10] A. Moradewicz, "Study of wireless energy transmission systems using inductive coupling", *Proc. Int. Conf. PELINCEC*, CD-ROM (2005).

[11] A. Moradewicz and M.P. Kazmierkowski, "Resonant converter based contactless power supply for robots and manipulators", *J. Automation, Mobile Robotics & Intelligent Systems* 2 (3), 20–25 (2008).

[12] K. O'Brien, G. Scheible, and H. Gueldner, "Analysis of wireless power supplies for industrial automation systems", *Proc. IEEE Industrial Electronics Conf. IECON*, CD-ROM (2003).

[13] Ch-S. Wang, O.H. Stielau, and G.A. Covic, "Design considerations for contactless electric vehicle battery charger", *IEEE Trans. on Industrial Electronics* 52 (5), 1308–1313 (2005).

[14] Z. Chen, X. Zhang, and J. Pan, "An integrated inverter for a single-phase single-stage grid connected PV system based on Z-source", *Bull. Pol Ac.: Tech.* 55 (3), 263–272 (2007).

[15] Z. Kaczmarczyk, "A novel phase-shift full-bridge converter with voltage-doubler and decoupling integrated magnetics in PV system", *Bull. Pol Ac.: Tech.* 56 (3), 285–293 (2008).

[16] W. Erickson, *Fundamentals of Power Electronics*, Kluwer Academic Publisher, New York, 1999.

[17] Y. Jiang, Z. Chen, J. Pan, X. I. Zhao, and P. Lee, "A novel phase-shift full-bridge converter with voltage-doubler and decoupling integrated magnetics in PV system", *Bull. Pol Ac.: Tech.* 56 (3), 285–293 (2008).

[18] P. Antoniewicz and M.P. Kazmierkowski, "Predictive direct power control of three-phase boost rectifier", *Bull. Pol Ac.: Tech.* 54 (2), 447–454 (2006).